Physics Letters B 753 (2016) 191–198

Contents lists available at ScienceDirect

Physics Letters B

www.elsevier.com/locate/physletb

Updating neutrino magnetic moment constraints

B.C. Cañas [a], O.G. Miranda [a,*], A. Parada [b], M. Tórtola [c], J.W.F. Valle [c]

[a] Departamento de Física, Centro de Investigación y de Estudios Avanzados del IPN, Apdo. Postal 14-740, 07000 Mexico, DF, Mexico
[b] Universidad Santiago de Cali, Campus Pampalinda, Calle 5 No. 6200, 760001, Santiago de Cali, Colombia
[c] AHEP Group, Institut de Física Corpuscular – C.S.I.C./Universitat de València, Parc Cientific de Paterna, C/Catedratico José Beltrán, 2, E-46980 Paterna (València), Spain

ARTICLE INFO

Article history:
Received 9 October 2015
Received in revised form 1 December 2015
Accepted 4 December 2015
Available online 8 December 2015
Editor: W. Haxton

ABSTRACT

In this paper we provide an updated analysis of the neutrino magnetic moments (NMMs), discussing both the constraints on the magnitudes of the three transition moments Λ_i and the role of the CP violating phases present both in the mixing matrix and in the NMM matrix. The scattering of solar neutrinos off electrons in Borexino provides the most stringent restrictions, due to its robust statistics and the low energies observed, below 1 MeV. Our new limit on the effective neutrino magnetic moment which follows from the most recent Borexino data is $3.1 \times 10^{-11}\mu_B$ at 90% C.L. This corresponds to the individual transition magnetic moment constraints: $|\Lambda_1| \leq 5.6 \times 10^{-11}\mu_B$, $|\Lambda_2| \leq 4.0 \times 10^{-11}\mu_B$, and $|\Lambda_3| \leq 3.1 \times 10^{-11}\mu_B$ (90% C.L.), irrespective of any complex phase. Indeed, the incoherent admixture of neutrino mass eigenstates present in the solar flux makes Borexino insensitive to the Majorana phases present in the NMM matrix. For this reason we also provide a global analysis including the case of reactor and accelerator neutrino sources, presenting the resulting constraints for different values of the relevant CP phases. Improved reactor and accelerator neutrino experiments will be needed in order to underpin the full profile of the neutrino electromagnetic properties.

1. Introduction

Neutrino physics has now reached the precision age characterizing a mature science. Underpinning the origin of neutrino mass remains an open challenge, whose investigation could help us find our way towards the ultimate theory of everything [1]. Indeed, the search for new phenomenological signatures associated to massive neutrinos may yield valuable clues towards the structure of the electroweak theory beyond the Standard Model (SM). Although the field is very active, most of the experimental efforts are devoted to explore the neutrino mass pattern through the study of oscillations [2,3]. However it is also of great importance to investigate the implications of dimension-6 non-standard interactions [4–6] as well as electromagnetic properties of the neutrinos [7–15]. Here we focus on the latter, which has also been a lively subject of phenomenological research in the last few years [16–21]. Indeed, different experiments have set constraints coming mainly from reactor neutrino studies [22,23] as well as from solar neutrino data [16,17]. Future tests from experiments measuring coherent neutrino-nucleus scattering are expected to improve the current bounds on neutrino electromagnetic properties [24–28]. Most of the constraints reported by the experiments refer to the case of a Dirac neutrino magnetic moment, despite the fact that Majorana neutrinos are better motivated from the theoretical point of view [29]. However the Majorana case has been considered in Refs. [17,18] where a more complete analysis was performed. Other recent theoretical studies of the neutrino magnetic moment in the case of Majorana neutrinos can be found in [30] and [31].

In this article we perform a combined analysis of reactor, accelerator and solar neutrino data, in order to obtain constraints on the Majorana neutrino transition magnetic moments. We include the most recent results from the TEXONO reactor experiment [23], as well as the recent results from the Borexino experiment [32]. Data from the reactor experiments Krasnoyarsk [33], Rovno [34] and MUNU [35] as well as the accelerator experiments LAMPF [36] and LSND [37] are also included. Moreover, in our analysis we take into account the updated values of the neutrino mixing parameters as determined in global oscillation fits [2], including the value of θ_{13} implied by Daya-Bay [38,39] and RENO reactor data [40], as

* Corresponding author.
E-mail addresses: bcorduz@fis.cinvestav.mx (B.C. Cañas), omr@fis.cinvestav.mx (O.G. Miranda), alexander.parada00@usc.edu.co (A. Parada), mariam@ific.uv.es (M. Tórtola), valle@ific.uv.es (J.W.F. Valle).
URL: http://astroparticles.es/ (J.W.F. Valle).

http://dx.doi.org/10.1016/j.physletb.2015.12.011

well as accelerator data [41]. Moreover, we pay attention to the role of the, yet unknown, leptonic CP violating phases.

2. The neutrino magnetic moment

In this section we will establish the notation used in the description of neutrino magnetic moments. This will be very important in order to understand the constraints and the differences between Dirac and Majorana cases. For the general Majorana case we have the effective Hamiltonian [9]

$$H^M_{em} = -\frac{1}{4}\nu_L^T C^{-1}\,\lambda\,\sigma^{\alpha\beta}\nu_L F_{\alpha\beta} + h.c., \tag{1}$$

where $\lambda = \mu - id$ is an antisymmetric complex matrix $\lambda_{\alpha\beta} = -\lambda_{\beta\alpha}$, so that $\mu^T = -\mu$ and $d^T = -d$ are imaginary. Hence, three complex or six real parameters are needed to describe the Majorana neutrino case.

On the other hand, for the particular case[1] of Dirac neutrino magnetic moments, the corresponding Hamiltonian is given by [42]

$$H^D_{em} = \frac{1}{2}\bar{\nu}_R\,\lambda\,\sigma^{\alpha\beta}\nu_L F_{\alpha\beta} + h.c., \tag{2}$$

with $\lambda = \mu - id$ being an arbitrary complex matrix. Hermiticity now implies that μ and d obey $\mu = \mu^\dagger$ and $d = d^\dagger$. We should stress that experimental measurements usually constrain some process-dependent effective parameter combination. Even in the case of laboratory neutrino experiments, where the initial neutrino flux is fixed to have a well determined given flavor, there is no sensitivity to the final neutrino state and therefore several possibilities must be envisaged. For the case of solar neutrino experiments, one needs to take into account that the original electron neutrino flux experiences oscillations on its way to the Earth. Therefore, most of the neutrino magnetic moment constraints discussed in the literature correspond to restrictions upon some process-dependent effective parameter. The latter is expressed in terms of the fundamental parameters describing the transition magnetic moments and their phases, as well as the neutrino mixing parameters.

From now on we are concerned with the case of three "genuine" active Majorana neutrinos. As already mentioned, the Dirac case, with three active plus three sterile neutrinos, would be a particular case of the six-dimensional Majorana neutrino picture, in which the standard Dirac magnetic moment is viewed as a transition moment connecting an "active" with a "sterile" neutrino.

Before we express our results in terms of a general phenomenological notation, we can illustrate the general features of the neutrino magnetic moment for the simplest model, namely we consider the case of Majorana neutrino masses in the standard $SU(2)_L \otimes U(1)_Y$ gauge theory [10], in which case the charged current contribution gives

$$\mu_{ij} = \frac{3eG_F}{16\pi^2\sqrt{2}}(m_{\nu i} + m_{\nu j})\sum_{\alpha=e}^{\tau} i\mathcal{I}m\left[U^*_{\alpha i}U_{\alpha j}\left(\frac{m_{l\alpha}}{M_W}\right)^2\right]. \tag{3}$$

Notice that, in this example, if the masses of the charged leptons were degenerate, then the off-diagonal transition magnetic moments would be zero, due to the assumed unitarity of the U matrix. However, in reality, this is not the case and the transition magnetic moments are non-zero. Moreover, the phases in μ_{ij} will be the same as present in the lepton mixing matrix U and, therefore, could in principle be reconstructed. However, due to the proportionality with the neutrino mass, the magnetic moments expected just from the $SU(2)_L \otimes U(1)_Y$ gauge sector are too small to be phenomenologically relevant.

Although enhanced Majorana transition moments are possible in extended theories, this discussion is beyond the scope of this paper. However, we quote, as an illustrative example, the case of an extended model with a charged scalar singlet η^+ suggested in Ref. [43]. In this case the neutrino transition magnetic moment would be dominated by a charged Higgs boson contribution, and has been estimated as

$$\mu_{ij} = e\sum_k \frac{f_{ki}g^\dagger_{kj} + g_{ik}f^\dagger_{kj}}{32\pi^2}\frac{m_{lk}}{m^2{}_\eta}\left(\ln\frac{m^2_\eta}{m^2_{l_k}} - 1\right). \tag{4}$$

Indeed, in principle this scalar contribution could be higher than the one discussed in Eq. (3). Note that in the case of Higgs-dominated NMM one could, in principle, introduce new CP phases in addition to those characterizing the lepton mixing matrix.

The above discussion could be translated into a more phenomenological approach in which the Dirac NMM is described by an arbitrary complex matrix $\lambda = \mu - id$ ($\tilde{\lambda}$) in the flavor (or mass) basis, while for the Majorana case the matrix λ takes the form

$$\lambda = \begin{pmatrix} 0 & \Lambda_\tau & -\Lambda_\mu \\ -\Lambda_\tau & 0 & \Lambda_e \\ \Lambda_\mu & -\Lambda_e & 0 \end{pmatrix},$$

$$\tilde{\lambda} = \begin{pmatrix} 0 & \Lambda_3 & -\Lambda_2 \\ -\Lambda_3 & 0 & \Lambda_1 \\ \Lambda_2 & -\Lambda_1 & 0 \end{pmatrix}, \tag{5}$$

where we have used the notation $\lambda_{\alpha\beta} = \varepsilon_{\alpha\beta\gamma}\Lambda_\gamma$, where we assume the transition magnetic moments Λ_α and Λ_i to be complex parameters: $\Lambda_\alpha = |\Lambda_\alpha|e^{i\zeta_\alpha}$, $\Lambda_i = |\Lambda_i|e^{i\zeta_i}$. We now turn to the issue of extracting information on these parameters from experiment.

2.1. The effective neutrino magnetic moment

For the particular case of neutrino scattering off electrons, the differential cross section for the magnetic moment contribution will be given by

$$\left(\frac{d\sigma}{dT}\right)_{em} = \frac{\pi\alpha^2}{m_e^2\mu_B^2}\left(\frac{1}{T} - \frac{1}{E_\nu}\right)\mu_\nu{}^2, \tag{6}$$

where μ_ν is an effective magnetic moment accounting for the NMM contribution to the scattering process.

The effective magnetic moment μ_ν is defined in terms of the components of the NMM matrix in Eq. (5). In the flavor basis this can be written as [17,42]

$$(\mu^F_\nu)^2 = a^\dagger_-\lambda^\dagger\lambda a_- + a^\dagger_+\lambda\lambda^\dagger a_+ \tag{7}$$

where a_- and a_+ denote the negative and positive helicity neutrino amplitudes, respectively. One finds

$$\begin{aligned}(\mu^F_\nu)^2 = {} & |a^1_-\Lambda_\mu - a^2_-\Lambda_e|^2 + |a^1_-\Lambda_\tau - a^3_-\Lambda_e|^2 \\ & + |a^2_-\Lambda_\tau - a^3_-\Lambda_\mu|^2 + |a^1_+\Lambda_\mu - a^2_+\Lambda_e|^2 \\ & + |a^1_+\Lambda_\tau - a^3_+\Lambda_e|^2 + |a^2_+\Lambda_\tau - a^3_+\Lambda_\mu|^2.\end{aligned} \tag{8}$$

In order to write the expression for the effective neutrino magnetic moment in the mass basis we will need the transformations

$$\tilde{a}_- = U^\dagger a_-, \qquad \tilde{a}_+ = U^T a_+, \qquad \tilde{\lambda} = U^T\lambda U, \tag{9}$$

leading to the expression

[1] A Dirac neutrino is equivalent to two Majorana neutrinos of same mass and opposite CP [29]. Indeed, in two-component form, the three Dirac neutrinos are described by a 6×6 transition moment matrix.

$$(\mu_\nu^M)^2 = \tilde{a}_-^\dagger \tilde{\lambda}^\dagger \tilde{\lambda} \tilde{a}_- + \tilde{a}_+^\dagger \tilde{\lambda} \tilde{\lambda}^\dagger \tilde{a}_+, \tag{10}$$

so that

$$\begin{aligned}(\mu_\nu^M)^2 = {} & |\tilde{a}_-^1 \Lambda_2 - \tilde{a}_-^2 \Lambda_1|^2 + |\tilde{a}_-^1 \Lambda_3 - \tilde{a}_-^3 \Lambda_1|^2 \\ & + |\tilde{a}_-^2 \Lambda_3 - \tilde{a}_-^3 \Lambda_2|^2 + |\tilde{a}_+^1 \Lambda_2 - \tilde{a}_+^2 \Lambda_1|^2 \\ & + |\tilde{a}_+^1 \Lambda_3 - \tilde{a}_+^3 \Lambda_1|^2 + |\tilde{a}_+^2 \Lambda_3 - \tilde{a}_+^3 \Lambda_2|^2, \end{aligned} \tag{11}$$

where $\tilde{a}_\pm^i$ denotes the i-th component of the $\tilde{a}_\pm$ vector.

Before starting the calculations of the effective Majorana magnetic moment parameter combination corresponding to the different experimental setups we would like to comment on the counting of relevant complex phases. First we write the three complex phases in the transition magnetic moment matrix as ζ_1, ζ_2 and ζ_3. From the leptonic mixing matrix we have another 3 CP-violating phases: the Dirac phase characterizing neutrino oscillations, δ, and the two Majorana phases involved in lepton number violating processes [29]. As noticed in Ref. [42], three of these six complex phases are irrelevant, as they can be reabsorbed in different ways. In what follows we give our results in terms of the Dirac CP phase δ and the relative difference between the transition magnetic moment phases, $\xi_1 = \zeta_3 - \zeta_2$, $\xi_2 = \zeta_3 - \zeta_1$, $\xi_3 = \zeta_2 - \zeta_1$, of which only two are independent.

2.1.1. Effective neutrino magnetic moment at reactor experiments

We now consider the effective neutrino magnetic moment parameter relevant for the case of reactor neutrinos. In this case we have an initial electron antineutrino flux, so that the only non-zero entry in the flavor basis will be $a_+^1 = 1$. Therefore, from Eq. (8) we get the following expression for the effective Majorana transition magnetic moment strength parameter describing reactor neutrino experiments:

$$(\mu_R^F)^2 = |\Lambda_\mu|^2 + |\Lambda_\tau|^2, \tag{12}$$

which in the mass basis leads to the expression

$$\begin{aligned}(\mu_R^M)^2 = {} & |\mathbf{\Lambda}|^2 - s_{12}^2 c_{13}^2 |\Lambda_2|^2 - c_{12}^2 c_{13}^2 |\Lambda_1|^2 - s_{13}^2 |\Lambda_3|^2 \\ & - 2 s_{12} c_{12} c_{13}^2 |\Lambda_1||\Lambda_2| \cos\delta_{12} \\ & - 2 c_{12} c_{13} s_{13} |\Lambda_1||\Lambda_3| \cos\delta_{13} \\ & - 2 s_{12} c_{13} s_{13} |\Lambda_2||\Lambda_3| \cos\delta_{23} \end{aligned} \tag{13}$$

where $c_{ij} = \cos\theta_{ij}$, $s_{ij} = \sin\theta_{ij}$ and $\delta_{12} = \xi_3$, $\delta_{23} = \xi_2 - \delta$, and $\delta_{13} = \delta_{12} - \delta_{23}$. As already noted, δ is the Dirac phase of the leptonic mixing matrix and $\xi_3 = \zeta_2 - \zeta_1$, $\xi_2 = \zeta_3 - \zeta_1$, are the relative phases introduced by the presence of the magnetic moment. This expression takes into account that θ_{13} is different from zero, and hence generalizes the previous result given in [17].

It is important to notice that the effective magnetic moment in Eq. (13) implies a degeneracy between the leptonic phase δ and those present in the neutrino transition magnetic moments, ξ_2 and ξ_3. As a result, it will not be possible to disentangle these phases without further independent experimental information.

In order to illustrate the dependence on the different relative phases δ_{ij} we show in Fig. 1 the value of the effective Majorana transition magnetic moment for three particular cases, in which the magnitude of one transition magnetic moment $|\Lambda_i|$ is assumed to vanish. This implies that the magnetic moment would depend only on one effective phase δ_{ij}. Comparing the three curves in Fig. 1, one sees a strong dependence on the phase δ_{12} (see solid black line) while, due to the smallness of $\sin\theta_{13}$, the value of the phases δ_{13} and δ_{23} has little impact on the magnitude of the effective magnetic moment μ_R^M.

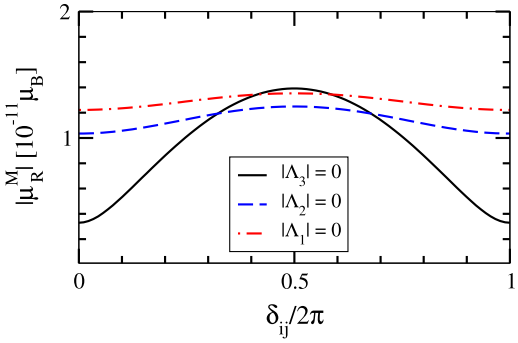

Fig. 1. Effective Majorana transition magnetic moment probed in reactor neutrino experiments, versus the relative phases δ_{ij} for three limiting cases where one of the absolute values $|\Lambda_k|$ vanishes.

2.1.2. Effective neutrino magnetic moment at accelerator experiments

Another relevant measurement for neutrino magnetic moment comes from accelerator-produced neutrinos arising from pion decays [36,37]. In this case, pion decay produces a muon neutrino, while the subsequent muon decay generates an electron neutrino plus a muon antineutrino. We can write the effective magnetic moment strength parameter in the flavor basis, considering for the moment the same proportion of ν_e, ν_μ and $\bar{\nu}_\mu$ ($a_-^1 = 1$, $a_-^2 = 1$, $a_+^2 = 1$):

$$(\mu_A^F)^2 = |\mathbf{\Lambda}|^2 + |\Lambda_e|^2 + 2|\Lambda_\tau|^2 - 2|\Lambda_\mu||\Lambda_e| \cos\eta, \tag{14}$$

where $|\mathbf{\Lambda}|^2 = |\Lambda_e|^2 + |\Lambda_\mu|^2 + |\Lambda_\tau|^2$ and $\eta = \zeta_e - \zeta_\mu$ is the relative phase between the transition magnetic moments Λ_e and Λ_μ.

The corresponding expression for the effective neutrino magnetic moment strength parameter in the mass basis, for $\theta_{13} = 0$ will be given by

$$\begin{aligned}(\mu_A^M)^2 = {} & |\Lambda_1|^2[2 - (c_{23}^2 - s_{23}^2) s_{12}^2 + 2 s_{12} c_{12} c_{23}] \\ & + |\Lambda_2|^2[2 - (c_{23}^2 - s_{23}^2) c_{12}^2 - 2 s_{12} c_{12} c_{23}] \\ & + |\Lambda_3|^2[1 + 2 c_{23}^2] \\ & + 2|\Lambda_1||\Lambda_2| \cos\xi_3 [s_{12} c_{12} (c_{23}^2 - s_{23}^2) - (c_{12}^2 - s_{12}^2) c_{23}] \\ & + 2|\Lambda_1||\Lambda_3| \cos\xi_2 [-c_{12} s_{23} + 2 s_{12} s_{23} c_{23}] \\ & + 2|\Lambda_2||\Lambda_3| \cos(\xi_3 - \xi_2)[-s_{12} s_{23} - 2 c_{12} s_{23} c_{23}] \end{aligned} \tag{15}$$

As expected, the Dirac CP phase δ present in oscillations does not enter in this expression, and therefore only the two Majorana phases from the NMM matrix ξ_2 and ξ_3 are present. Note however that in our numerical analysis we have used the full expression with $\theta_{13} \neq 0$, as

$$\begin{aligned}\left(\mu_A^M\right)^2 = {} & |\Lambda_1|^2 \big[\sin 2\theta_{12} c_{13} c_{23} \\ & + c_{12}^2 \left(2 c_{23}^2 + \sin 2\theta_{13} s_{23} \cos\delta\right) \\ & + c_{13}^2 \left(s_{12}^2 + 2 s_{23}^2\right) + s_{13} \left(s_{13} + 2 s_{12}^2 s_{13} s_{23}^2\right. \\ & \left. - \sin 2\theta_{12} \sin 2\theta_{23} \cos\delta\right)\big] \\ & + \frac{1}{4} |\Lambda_2|^2 \big[8 - \cos 2\theta_{23} \left(1 + 3\cos 2\theta_{12} + 2\cos 2\theta_{13} s_{12}^2\right) \\ & + 4 s_{12}^2 \sin 2\theta_{13} s_{23} \cos\delta \\ & + 4 \sin 2\theta_{12} \left(-c_{13} c_{23} + s_{13} \sin 2\theta_{23} \cos\delta\right)\big] \\ & + |\Lambda_3|^2 \left(2 + c_{13}^2 \cos 2\theta_{23} - \sin 2\theta_{13} s_{23} \cos\delta\right) \\ & + 2|\Lambda_1||\Lambda_2| \big\{\cos\xi_3 \big[-c_{12}^2 c_{13} c_{23} \\ & + c_{23} \left(s_{12}^2 c_{13} + \sin 2\theta_{12} c_{23}\right)\end{aligned}$$

$$
\begin{aligned}
&+ s_{12}c_{12}\left(-1+\cos 2\theta_{23}s_{13}^2+\sin 2\theta_{13}s_{23}\cos\delta\right)\Big]\\
&+ s_{13}\sin 2\theta_{23}(\cos 2\theta_{12}\cos\delta\cos\xi_3+\sin\delta\sin\xi_3)\Big\}\\
&+ |\Lambda_1||\Lambda_3|\Big\{2\cos(\xi_2-\delta)\\
&\times(-c_{12}c_{13}\cos 2\theta_{23}+s_{12}c_{23})s_{13}\\
&+ 2\Big[c_{13}\cos\xi_2(-c_{12}c_{13}+2s_{12}c_{23})\\
&+ c_{12}s_{13}^2\cos(\xi_2-2\delta)\Big]s_{23}\Big\}\\
&- 2|\Lambda_2||\Lambda_3|\Big\{\frac{1}{2}s_{12}\cos(\xi_1-\delta)(\cos 2\theta_{23}\sin 2\theta_{13}\\
&+ 2\cos 2\theta_{13}s_{23}\cos\delta)\\
&+ c_{12}\Big[c_{23}s_{13}\cos(\xi_1-\delta)+c_{13}\sin 2\theta_{23}\cos\xi_1\Big]\\
&+ s_{12}s_{23}\sin\delta\sin(\delta-\xi_1)\Big\} \qquad (16)
\end{aligned}
$$

Notice that we have used here the phase $\xi_1=\xi_2-\xi_3$. Although this is not an independent phase, it is helpful to simplify the previous formula. Therefore, the final expression is given in terms of the three independent phases δ, ξ_2 and ξ_3. One can check that in the limit $\theta_{13}=0$, the expression in Eq. (15) is recovered.

2.1.3. Effective neutrino magnetic moment in Borexino

Here we calculate the effective magnetic moment strength parameter relevant for experiments measuring solar neutrinos through their scattering with electrons, like Borexino.[2] In this case, the electron neutrinos originally produced in the solar interior undergo flavor oscillation and they arrive to the Earth detector as an incoherent sum of mass eigenstates. Using the well-justified approximation where [17]

$$
\begin{aligned}
P_{e3}^{3\nu} &= \sin^2\theta_{13},\\
P_{e1}^{3\nu} &= \cos^2\theta_{13}P_{e1}^{2\nu},\\
P_{e2}^{3\nu} &= \cos^2\theta_{13}P_{e2}^{2\nu}, \qquad (17)
\end{aligned}
$$

with $P_{ej}^{2\nu}$ $(j=1,2)$ being the effective two-neutrino oscillation probabilities for solar neutrinos, we arrive to the effective neutrino magnetic moment strength parameter in the mass basis,

$$
\begin{aligned}
(\mu_{\rm sol}^M)^2 &= |\mathbf{\Lambda}|^2-c_{13}^2|\Lambda_2|^2+(c_{13}^2-1)|\Lambda_3|^2\\
&\quad + c_{13}^2P_{e1}^{2\nu}(|\Lambda_2|^2-|\Lambda_1|^2), \qquad (18)
\end{aligned}
$$

where the unitarity condition, $P_{e1}^{2\nu}+P_{e2}^{2\nu}=1$, has also been assumed. The calculation of this expression in the flavor basis is more complicated due to presence of the neutrino transition probabilities and therefore we do not include it here.

As we can see from Eq. (18), the expression of the effective magnetic moment for solar neutrinos is independent of any phase, as has already been noticed [17]. Here we take into account the non-zero value of θ_{13} for the first time in this kind of analysis. Taking advantage of the previous equation we obtain constraints on the individual neutrino transition magnetic moments. After obtaining the neutrino magnetic moment expressions for the case of $\theta_{13}\neq 0$, we now turn our attention to the relevant experiments for our analysis.

[2] The same result will apply for the Super-Kamiokande experiment, not included here due to its smaller sensitivity to the neutrino magnetic moment [17].

3. Neutrino data analysis

Having evaluated the effective neutrino magnetic moment strength parameter for reactor, accelerator and solar neutrino experiments, we are ready to perform a combined analysis of the experimental data in order to get constraints on the three different transition magnetic moments Λ_i. In order to perform this analysis we make some assumptions on the phases δ, ξ_2 and ξ_3. In the next section we will describe the data used in the fit and show the results. We now briefly describe the statistical analysis performed in this article.

3.1. Reactor antineutrinos

We start by describing the reactor antineutrino experiments. They use the antineutrino flux coming from a nuclear reactor, in combination with a detector sensitive to the electron antineutrino scattering off electrons. The total number of events (in the i-th bin) in these experiments is given by

$$
N_R^i=\kappa\int dE_\nu\int dT\int_{T_i}^{T_{i+1}}dT'\lambda(E_\nu)\frac{d\sigma}{dT}(E_\nu,T,\mu)R(T,T'), \qquad (19)
$$

where the integrals run over the detected electron recoil energy T', the real recoil energy T, and the neutrino energy E_ν. T_i and T_{i+1} are the minimum and maximum energy of the i-th bin, respectively. The parameter κ stands for the product of the total number of targets times the total antineutrino flux times the total exposure time of the experimental run and $\lambda(E_\nu)$ is the antineutrino energy spectrum coming from the nuclear reactor [44,45]. Some of the experiments under consideration reported their resolution function $R(T,T')$, given by

$$
R(T,T')=\frac{1}{\sqrt{4\pi}\sigma}\exp\left(\frac{-(T-T')^2}{2\sigma^2}\right), \qquad (20)
$$

where σ stands for the error in the kinetic energy determination. When the information on this resolution function is not available, we have assumed perfect energy resolution and taken it as a delta function: $R(T,T')=\delta(T-T')$.

Finally, the standard differential cross section for the process of $\bar{\nu}_e$-electron scattering is given by

$$
\frac{d\sigma}{dT}=\frac{2G_F^2m_e}{\pi}\left[g_R^2+g_L^2(1-\frac{T}{E_\nu})^2-g_Lg_Rm_e\frac{T}{E_\nu^2}\right], \qquad (21)
$$

where m_e is the electron mass and G_F is the Fermi constant. For this process, at tree level, the coupling constants $g_{L,R}$ are given by $g_L=1/2+\sin^2\theta_{\rm W}$ and $g_R=\sin^2\theta_{\rm W}$. The assumed non-zero neutrino magnetic moment yields a new contribution to the cross section, given by

$$
\left(\frac{d\sigma}{dT}\right)_{em}=\frac{\pi\alpha^2}{m_e^2}\left(\frac{1}{T}-\frac{1}{E_\nu}\right)\mu_R{}^2, \qquad (22)
$$

where $\mu_R=\mu_R^{F,M}$ is the reactor effective neutrino magnetic moment, either in the mass or flavor basis, as already discussed in Eqs. (12) and (13). This gives rise to an additional neutrino signal at reactor experiments. Finally, we perform our statistical analysis using the following χ^2 function:

$$
\chi^2=\sum_{i=1}^{N_{bin}}\left(\frac{O_R^i-N_R^i(\mu_R)}{\Delta_i}\right)^2, \qquad (23)
$$

where O_R^i and N_R^i are the observed number of events and the predicted number of events in the presence of an effective magnetic

Table 1
90% C.L. limits (95% C.L. for Rovno) on the effective neutrino magnetic moment from reactor and accelerator data.

Experiment	Bounds
Reactors	**[Expression in Eqs. (12)–(13)]**
KRASNOYARSK [33]	$\mu_{\bar{\nu}_e} \leq 2.7 \times 10^{-10} \mu_B$
ROVNO [34]	$\mu_{\bar{\nu}_e} \leq 1.9 \times 10^{-10} \mu_B$
MUNU [35]	$\mu_{\bar{\nu}_e} \leq 1.2 \times 10^{-10} \mu_B$
TEXONO [23]	$\mu_{\bar{\nu}_e} \leq 2.0 \times 10^{-10} \mu_B$
Accelerators	**[Expression in Eqs. (14)–(16)]**
LAMPF [36]	$\mu_{\nu_e} \leq 7.3 \times 10^{-10} \mu_B$
LAMPF [36]	$\mu_{\nu_\mu} \leq 5.1 \times 10^{-10} \mu_B$
LSND [37]	$\mu_{\nu_e} \leq 1.0 \times 10^{-9} \mu_B$
LSND [37]	$\mu_{\nu_\mu} \leq 6.5 \times 10^{-10} \mu_B$

moment μ_R at the i-th bin, respectively. Here Δ_i is the statistical error at each bin.

In our analysis, we have used the experimental results reported by Krasnoyarsk [33], Rovno [34], MUNU [35], and TEXONO [23] reactor experiments. As a first step we have calibrated our numerical analysis by reproducing the constraints on the effective neutrino magnetic moment reported by each experiment. To do this we performed an analysis as similar as possible to the original references, using the antineutrino spectrum description available at the time of the corresponding experiment as well as the antineutrino electron cross section. Afterwards, we have recalculated our limits on the NMM by introducing the new antineutrino reactor spectrum. Our results on reactor neutrino experiments are summarized in the upper part of Table 1.

Although it is not listed in Table 1, we have also analyzed the case of the GEMMA [46] experiment. In this case there is no detection of the SM signal and therefore, the statistical analysis is a bit different from what we have described above. It is important to notice that this experiment gives a stronger constraint compared with other reactor experiments ($\mu_{\bar{\nu}_e} \leq 2.9 \times 10^{-11} \mu_B$). However, the different statistical treatment employed to analyze GEMMA's data makes it difficult to establish a direct comparison with the remaining reactor results.

3.2. Accelerator data

For the case of accelerator neutrinos we have considered the experimental data reported by the LAMPF [36] and LSND [37] collaborations. The expected number of events for electron and muon neutrinos is calculated as

$$N_A = \int dE_\nu \int_{T_i}^{T_f} dT' \lambda(E_\nu) \frac{d\sigma}{dT}(E_\nu, T', \mu), \tag{24}$$

where A refers to the type of event (ν_e, ν_μ or $\bar{\nu}_\mu$), E_ν corresponds to the neutrino energy, T' is the electron recoil energy, and $\lambda(E_\nu)$ is the neutrino energy spectrum from the accelerator experiments [36,37]. The statistical analysis is similar to the one for reactor antineutrinos described in the previous subsection. As a first step we try to reproduce the individual limits on the magnetic moment of electron and muon neutrinos reported by the experimental collaborations. To do this we have used the χ^2 function given by Eq. (23), comparing the expected event number reported by the experiments with the calculated number of events. The limits on the muon and electron neutrino magnetic moments are derived taking into account the following relations for the effective neutrino magnetic moment (see Refs. [36] and [37] for details): $\mu^2_{\nu_e} + \alpha \mu^2_{\nu_\mu} < \mu^2_{eff}$, where α stands for the rate between muon and electron neutrinos in the detector. This ratio is expected to be equal to two as first approximation, since each pion decay produces a muon antineutrino plus a muon neutrino plus an electron neutrino. The values reported by the experimental collaborations are $\alpha = 2.1$ for LAMPF [36] and $\alpha = 2.4$ for LSND [37]. The limits on the effective neutrino magnetic moment derived from LAMPF and LSND data are reported in the lower part of Table 1. For the more complete analysis including the complex phases in the neutrino magnetic moment matrix we take $\alpha = 2$, as included in Eqs. (14)–(16).

Table 2
90% C.L. limits on the effective neutrino magnetic moment from Borexino data. We show for comparison the constraint previously reported and the bound obtained in this work.

Experiment	Previous limit [52]	This work	Full expression
Borexino	$\mu_\nu \leq 5 \times 10^{-11} \mu_B$	$\mu_\nu \leq 3.1 \times 10^{-11} \mu_B$	Eq. (18)

3.3. Borexino data

The Borexino experiment has successfully measured a large part of the neutrino flux spectrum coming from the Sun [47–50] and has set limits on the effective neutrino magnetic moment by using their observations of the Beryllium solar neutrino line [51,52]. In this paper we will consider the more recent measurements of the Beryllium solar flux reported in Ref. [32] in order to obtain a stronger constraint.

For reactor and accelerator experiments, our statistical analysis followed the covariant approach. In the case of the Borexino, however, we have adopted the pull approach [53]. Focusing on the Beryllium neutrino flux, the expected number of events at the i-th bin, N_i^{th}, will be given by

$$N_i^{th} = \kappa \int \frac{d\sigma}{dT_e}(E_\nu, T_e) R(T_e, T'_e) dT_e dT'_e + N_i^{bg}, \tag{25}$$

where N_i^{bg} represents the number of expected background events at the considered energy bin. Here κ stands for the product of the number of target electrons, the detection time window (740.7 days in this case), and the total Beryllium neutrino flux. T_e is the real electron kinetic energy and T'_e is the reconstructed one. The energy resolution function $R(T_e, T'_e)$ of the experiment is given by

$$R(T_e, T'_e) = \frac{1}{\sqrt{2\pi}\sigma^2} \exp\left(\frac{(T_e - T'_e)^2}{2\sigma^2}\right) \tag{26}$$

with $\sigma/T_e = 0.06\sqrt{T_e/\text{MeV}}$ [54]. Finally the differential cross section is given by

$$\frac{d\sigma_\alpha}{dT_e}(E_\nu, T_e) = \overline{P}_{ee} \frac{d\sigma_e}{dT_e}(E_\nu, T_e) + (1 - \overline{P}_{ee}) \frac{d\sigma_{\mu-\tau}}{dT_e}(E_\nu, T_e), \tag{27}$$

where the average survival electron–neutrino probability for the Beryllium line, $\overline{P}_{ee}$, determines the flavor composition of the neutrino flux detected in the experiment. According to the most recent analysis of solar neutrino data in Ref. [2] (excluding Borexino data to avoid any correlation with the present analysis) this value is set to $\overline{P^{\text{th}}_{ee}} = 0.54 \pm 0.03$.

In order to explore the sensitivity of the Borexino experiment to the neutrino magnetic moments, we include the new contribution to the differential cross section in Eq. (27):

$$\left(\frac{d\sigma}{dT}\right)_{em} = \frac{\pi \alpha^2}{m_e^2 \mu_B^2} \left(\frac{1}{T} - \frac{1}{E_\nu}\right) {\mu_{\text{sol}}}^2, \tag{28}$$

where μ_{sol} is the effective magnetic moment strength parameter relevant for the Borexino solar neutrino experiment derived in

Table 3
90% C.L. limits on the neutrino magnetic moment components in the mass basis, Λ_i, from reactor, accelerator, and solar data from Borexino. In this particular analysis we constrain one parameter at a time, setting all other magnetic moment parameters and phases to zero.

Experiment	$\lvert\Lambda_1\rvert$	$\lvert\Lambda_2\rvert$	$\lvert\Lambda_3\rvert$
KRASNOYARSK	$4.7\times10^{-10}\mu_B$	$3.3\times10^{-10}\mu_B$	$2.8\times10^{-10}\mu_B$
ROVNO	$3.0\times10^{-10}\mu_B$	$2.1\times10^{-10}\mu_B$	$1.8\times10^{-10}\mu_B$
MUNU	$2.1\times10^{-10}\mu_B$	$1.5\times10^{-10}\mu_B$	$1.3\times10^{-10}\mu_B$
TEXONO	$3.4\times10^{-10}\mu_B$	$2.4\times10^{-10}\mu_B$	$2.0\times10^{-10}\mu_B$
GEMMA	$5.0\times10^{-11}\mu_B$	$3.5\times10^{-11}\mu_B$	$2.9\times10^{-11}\mu_B$
LSND	$6.0\times10^{-10}\mu_B$	$8.1\times10^{-10}\mu_B$	$7.0\times10^{-10}\mu_B$
LAMPF	$4.5\times10^{-10}\mu_B$	$6.2\times10^{-10}\mu_B$	$5.3\times10^{-10}\mu_B$
Borexino	$5.6\times10^{-11}\mu_B$	$4.0\times10^{-11}\mu_B$	$3.1\times10^{-11}\mu_B$

Eq. (18) in the mass basis. This yields a new contribution to the expected number of events, which will determine the sensitivity to the presence of a neutrino magnetic moment.

With the expected event number, we have fitted our predictions to the experimental data in the statistical analysis. There we have considered the Borexino systematic errors associated to the fiducial mass ratio uncertainty ($\pi_{vol} = 6\%$), the energy scale uncertainty ($\pi^b_{scl} = 1\%$) and the energy resolution uncertainty ($\pi_{res} = 10\%$). We have also included in the fit the electron–neutrino survival probability $\overline{P}_{ee}$ as a free parameter (using the value of $\overline{P^{\rm th}_{ee}}$ given above as a prior) with the corresponding penalty in the χ^2 function. The constraint we have obtained for the effective neutrino magnetic moment using the latest Borexino data is given in Table 2. For comparison, we have also included in the table the previous bound, derived by the Borexino Collaboration in Ref. [52]. Note that our updated limit is comparable to the strongest bound reported by the GEMMA experiment and previously discussed in Sect. 3.1.

Using the expression of the effective neutrino magnetic moment in Borexino given by Eq. (18), we can also obtain limits on the individual elements of the transition magnetic moment matrix Λ_i. In this case, the calculations involve the neutrino oscillation probability $P^{2\nu}_{e1}$, which, as before, is considered in our χ^2 analysis as a free parameter with an associated penalty term. As a prior, we have considered again the value of the probability predicted by the analysis of all other solar neutrino data except Borexino, given by $P^{2\nu}_{e1}\big|_{\rm th} = 0.61 \pm 0.06$ [2]. Our results are summarized in the last row of Table 3.

4. Limits on the neutrino magnetic moment

In the previous section we have derived bounds on the effective neutrino magnetic moment parameter combinations relevant in reactor, accelerator and solar neutrino experiments. Our results are summarized in Tables 1 and 2. The most remarkable result is the limit obtained with the latest Borexino data: $\mu_{\rm sol} \leq 3.1\times10^{-11}\mu_B$, which is comparable to the constraint reported by the GEMMA [46] collaboration using reactor antineutrinos, $\mu_{\rm R} \leq 2.9\times10^{-11}\mu_B$.[3]

One can go one step further and make a combined analysis using all the data studied so far. This combined study cannot be done in terms of the effective magnetic moments, since they are different for each type of experiment, but we need to use a more general formalism, as the one we have discussed in section 2. We choose to work in the mass basis and hence we consider the NMM parameters Λ_1, Λ_2 and Λ_3. As a first step in our analysis, we take all elements as real, setting the complex phases to zero, and we also take one non-zero transition magnetic moment element Λ_i at a time. The results from this analysis are shown in Table 3, where one sees that the Borexino constraint is considerably stronger than the others, except for GEMMA, as we already commented.[4]

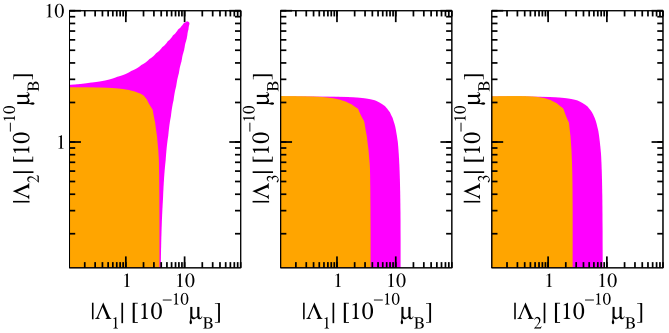

Fig. 2. 90% C.L. allowed regions for the transition neutrino magnetic moments in the mass basis from the reactor experiment TEXONO. The two-dimensional projections in the plane ($|\Lambda_i|$, $|\Lambda_j|$) have been calculated marginalizing over the third component. The magenta (outer) region is obtained for $\delta = 3\pi/2$ and $\xi_2 = \xi_3 = 0$, while the orange (inner) region appears for $\delta = 3\pi/2$, $\xi_2 = 0$ and $\xi_3 = \pi/2$. (For interpretation of the references to color in this figure legend, the reader is referred to the web version of this article.)

We have also considered a more complete analysis taking into account the role of the phases in the reactor and accelerator data. Notice that the effective magnetic moment for the Borexino experiment is independent of all the complex phases (see Eq. (18)) since solar neutrinos arrive to the Earth as an incoherent sum of mass eigenstates and therefore, no interference terms appear in the calculation. For the case of reactor neutrinos, we have performed a statistical analysis of TEXONO data [23] for different choices of the complex phases of Λ_i, ζ_i, and taking all transition magnetic moment amplitudes as non-zero. The results of this analysis are shown in Fig. 2. There we present the 90% C.L. allowed regions for the transition magnetic moments in the mass basis in the form of two-dimensional projections in the planes ($|\Lambda_i|$, $|\Lambda_j|$). In all cases the regions have been obtained marginalizing over the undisplayed parameter $|\Lambda_k|$. Concerning the complex phases, in the two cases considered we have fixed the mixing matrix CP phase δ to its currently preferred value [2]: $\delta = 3\pi/2$. For the complex phases in the transition magnetic moments we have considered two cases. The magenta (outer) region in Fig. 2 corresponds to the case with all phases equal to zero: $\xi_2 = \xi_3 = 0$ while the orange (inner) displayed region has been obtained for $\xi_2 = 0$ and $\xi_3 = \pi/2$. One can see in this plot the role of the CP phases, since the resulting restrictions on the transition magnetic moments $|\Lambda_1|$ and $|\Lambda_2|$ depend on the chosen phase combinations. Note, however, that in the two cases analyzed the bound on $|\Lambda_3|$ is practically unchanged, showing that in this particular case the complex phases are not very relevant. As discussed in Fig. 1, this is due to the fact that the terms involving simultaneously $|\Lambda_3|$ and any complex phase in the expression of the effective magnetic moment in Eq. (13) are proportional the small quantity $\sin\theta_{13}$ and therefore they are subdominant with respect to the real terms in μ^M_R.

Finally, we have performed a combined analysis of all the reactor and accelerator data discussed in this paper, for a particular choice of phases ($\delta = 3\pi/2$ and $\xi_i = 0$) and compared it with the corresponding χ^2 analysis of Borexino data. The results, shown in

[3] Both limits correspond to 90% C.L.

[4] Due to the complexity of the statistical analysis in GEMMA, here we have only translated their reported bound [46] into Λ_i by using Eq. (13), instead of including GEMMA data explicitly in the global analysis.

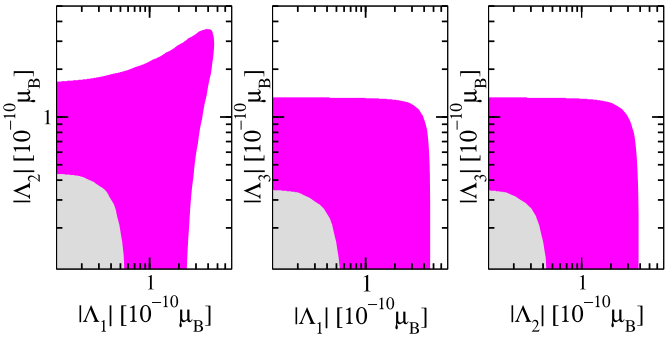

Fig. 3. 90% C.L. allowed regions for the transition neutrino magnetic moments in the mass basis. The result of this plot was obtained for the two parameters $|\Lambda_i|$ vs $|\Lambda_j|$ marginalizing over the third component. We show the result of a combined analysis of reactor and accelerator data with all phases set to zero except for $\delta = 3\pi/2$ (magenta region). We also show the result of the Borexino data analysis only, that is phase-independent (grey region). It is visible that Borexino data gives a more stringent constraint. See text for details.

Fig. 3, illustrate how Borexino is more sensitive in constraining the magnitude of the transition neutrino magnetic moments. Since the Borexino effective magnetic moment depends only on the square magnitudes of these transition magnetic moments, its constraints are in practice the same as those in the one-parameter-at-a-time analysis. In this sense, a detailed analysis of GEMMA data, not performed here, is not expected to give a result as robust as the one obtained with Borexino data. However, one should notice that future reactor and accelerator experiments are the only ones that could give information on individual transition magnetic moments as well as on the Majorana phases discussed here, an information inaccessible at Borexino. This information is crucial in certain analyses of the neutrino Majorana nature such as those recently performed in Refs. [30,31].

5. Conclusions

In this work we have analyzed the current status of the constraints on neutrino magnetic moments. We have presented a detailed discussion of the constraints on the absolute value of the transition magnetic moments, as well as the role of the CP phases, stressing the complementarity of different experiments. Thanks to the low energies observed, below 1 MeV, and its robust statistics, the Borexino solar experiment plays a very important role in constraining the electromagnetic neutrino properties. Indeed, it provides stringent constraints on the absolute magnitude of the transition magnetic moments, which we obtain as

$$
\begin{aligned}
|\Lambda_1| &\leq 5.6 \times 10^{-11}\mu_B\,,\\
|\Lambda_2| &\leq 4.0 \times 10^{-11}\mu_B\,,\\
|\Lambda_3| &\leq 3.1 \times 10^{-11}\mu_B\,.
\end{aligned}
\tag{29}
$$

However, the incoherent nature of the solar neutrino flux makes Borexino insensitive to the Majorana phases which characterize the transition moments matrix. Although less sensitive to the absolute value of the transition magnetic moment strengths, reactor and accelerator experiments provide the only chance to obtain a hint of the complex CP phases. We illustrate this fact by presenting the constraints resulting from our global analysis for different values of the relevant CP phases. Although less stringent than astrophysical limits say, from globular clusters [55,56] or searches for antineutrinos from the sun [57,58], laboratory limits are model independent and should be further pursued. Indeed, as we have illustrated, improved reactor and accelerator neutrino experiments will be crucial towards obtaining the detailed structure of the neutrino electromagnetic properties.

Acknowledgements

Work was supported by MINECO grants FPA2014-58183-P, Multidark CSD2009-00064 and SEV-2014-0398 (MINECO); by EPLANET, by the CONACYT grant 166639 (Mexico) and the PROMETEOII/2014/084 grant from Generalitat Valenciana. M. Tórtola is also supported by a Ramon y Cajal contract of the Spanish MINECO. The work of A. Parada was partially supported by Universidad Santiago de Cali under grant 935-621114-031.

References

[1] J.W. Valle, J.C. Romao, Neutrinos in High Energy and Astroparticle Physics, 1st ed., Wiley–VCH, Berlin, 2015.
[2] D. Forero, M. Tortola, J. Valle, Phys. Rev. D 90 (2014) 093006, arXiv:1405.7540.
[3] M. Maltoni, T. Schwetz, M. Tortola, J.W.F. Valle, New J. Phys. 6 (2004) 122, arXiv:hep-ph/0405172, this review gives a comprehensive set of references.
[4] O.G. Miranda, M.A. Tortola, J.W.F. Valle, J. High Energy Phys. 10 (2006) 008.
[5] J. Barranco, et al., Phys. Rev. D 73 (2006) 113001, arXiv:hep-ph/0512195.
[6] J. Barranco, et al., Phys. Rev. D 77 (2008) 093014, arXiv:0711.0698.
[7] A. Cisneros, Astrophys. Space Sci. 10 (1971) 87.
[8] K. Fujikawa, R. Shrock, Phys. Rev. Lett. 45 (1980) 963.
[9] J. Schechter, J.W.F. Valle, Phys. Rev. D 24 (1883) (1981);
J. Schechter, J.W.F. Valle, Phys. Rev. D 25 (283) (1982) (Erratum).
[10] P.B. Pal, L. Wolfenstein, Phys. Rev. D 25 (1982) 766.
[11] B. Kayser, Phys. Rev. D 26 (1982) 1662.
[12] J.F. Nieves, Phys. Rev. D 26 (1982) 3152.
[13] R.E. Shrock, Nucl. Phys. B 206 (1982) 359.
[14] E.K. Akhmedov, Phys. Lett. B 213 (1988) 64.
[15] C.-S. Lim, W.J. Marciano, Phys. Rev. D 37 (1988) 1368.
[16] J.F. Beacom, P. Vogel, Phys. Rev. Lett. 83 (1999) 5222, arXiv:hep-ph/9907383.
[17] W. Grimus, M. Maltoni, T. Schwetz, M.A. Tortola, J.W.F. Valle, Nucl. Phys. B 648 (2003) 376, arXiv:hep-ph/0208132.
[18] J. Barranco, et al., Phys. Rev. D 66 (2002) 093009, arXiv:hep-ph/0207326, v3 KamLAND-updated version.
[19] C. Giunti, A. Studenikin, arXiv:1403.6344, 2014.
[20] C. Giunti, K.A. Kouzakov, Y.-F. Li, A.V. Lokhov, A.I. Studenikin, et al., arXiv:1506.05387, 2015.
[21] J. Barranco, O. Miranda, C. Moura, A. Parada, Phys. Lett. B 718 (2012) 26, arXiv:1205.4285.
[22] H.B. Li, et al., TEXONO Collaboration, arXiv:hep-ex/0212003, 2002.
[23] M. Deniz, et al., TEXONO Collaboration, Phys. Rev. D 81 (2010) 072001, arXiv:0911.1597.
[24] H.T. Wong, H.-B. Li, J. Li, Q. Yue, Z.-Y. Zhou, J. Phys. Conf. Ser. 39 (2006) 266, arXiv:hep-ex/0511001, [344(2005)].
[25] H.T. Wong, Nucl. Phys. A 844 (2010) 229C.
[26] A. Bolozdynya, et al., arXiv:1211.5199, http://inspirehep.net/record/1203677/files/arXiv:1211.5199.pdf, 2012.
[27] T.S. Kosmas, O.G. Miranda, D.K. Papoulias, M. Tortola, J.W.F. Valle, Phys. Rev. D 92 (2015) 013011, arXiv:1505.03202.
[28] T.S. Kosmas, O.G. Miranda, D.K. Papoulias, M. Tortola, J.W.F. Valle, arXiv:1506.08377, 2015.
[29] J. Schechter, J.W.F. Valle, Phys. Rev. D 22 (1980) 2227.
[30] A.B. Balantekin, N. Vassh, Phys. Rev. D 89 (2014) 073013, arXiv:1312.6858.
[31] J.-M. Frère, J. Heeck, S. Mollet, Phys. Rev. D 92 (2015) 053002, arXiv:1506.02964.
[32] G. Bellini, et al., Phys. Rev. Lett. 107 (2011) 141302, arXiv:1104.1816.
[33] G. Vidyakin, V. Vyrodov, I. Gurevich, Y. Kozlov, V. Martemyanov, et al., JETP Lett. 55 (1992) 206.
[34] A.I. Derbin, et al., JETP Lett. 57 (1993) 768.
[35] Z. Daraktchieva, et al., MUNU, Phys. Lett. B 615 (2005) 153, arXiv:hep-ex/0502037.
[36] R.C. Allen, et al., Phys. Rev. D 47 (1993) 11.
[37] L.B. Auerbach, et al., LSND, Phys. Rev. D 63 (2001) 112001, arXiv:hep-ex/0101039.
[38] F. An, et al., DAYA-BAY Collaboration, Phys. Rev. Lett. 108 (2012) 171803, arXiv:1203.1669.
[39] F. An, et al., Daya Bay, Phys. Rev. Lett. 112 (2014) 061801, arXiv:1310.6732.
[40] J. Ahn, et al., RENO Collaboration, Phys. Rev. Lett. 108 (2012) 191802, arXiv:1204.0626.
[41] K. Abe, et al., T2K Collaboration, arXiv:1311.4750, 2013.
[42] W. Grimus, T. Schwetz, Nucl. Phys. B 587 (2000) 45, arXiv:hep-ph/0006028.
[43] M. Fukugita, T. Yanagida, Phys. Rev. Lett. 58 (1987) 1807.
[44] T. Mueller, D. Lhuillier, M. Fallot, A. Letourneau, S. Cormon, et al., Phys. Rev. C 83 (2011) 054615, arXiv:1101.2663.

[45] V. Kopeikin, L. Mikaelyan, V. Sinev, Phys. At. Nucl. 60 (1997) 172.
[46] A. Beda, V. Brudanin, V. Egorov, D. Medvedev, V. Pogosov, et al., Adv. High Energy Phys. 2012 (2012) 350150.
[47] C. Arpesella, et al., Borexino, Phys. Lett. B 658 (2008) 101, arXiv:0708.2251.
[48] G. Bellini, et al., Borexino, Phys. Rev. D 82 (2010) 033006, arXiv:0808.2868.
[49] G. Bellini, et al., Borexino, Phys. Rev. D 89 (2014) 112007, arXiv:1308.0443.
[50] G. Bellini, et al., BOREXINO, Nature 512 (2014) 383.
[51] H.O. Back, et al., Phys. Lett. B 563 (2003) 35.
[52] C. Arpesella, et al., Borexino, Phys. Rev. Lett. 101 (2008) 091302, arXiv:0805.3843.
[53] G.L. Fogli, E. Lisi, A. Marrone, D. Montanino, A. Palazzo, Phys. Rev. D 66 (2002) 053010, arXiv:hep-ph/0206162.
[54] M.C. Gonzalez-Garcia, M. Maltoni, J. Salvado, J. High Energy Phys. 05 (2010) 072, arXiv:0910.4584.
[55] G.G. Raffelt, Phys. Rev. Lett. 64 (1990) 2856.
[56] S. Arceo-Díaz, K.P. Schröder, K. Zuber, D. Jack, Astropart. Phys. 70 (2015) 1.
[57] O.G. Miranda, T.I. Rashba, A.I. Rez, J.W.F. Valle, Phys. Rev. D 70 (2004) 113002, arXiv:hep-ph/0406066.
[58] O.G. Miranda, T.I. Rashba, A.I. Rez, J.W.F. Valle, Phys. Rev. Lett. 93 (2004) 051304, arXiv:hep-ph/0311014.